

Biological Denitrification in Microbial Fuel Cells

PETER CLAUWAERT,[†]
KORNEEL RABAEY,^{†,‡}
PETER AELTERMAN,[†]
LIESJE DE SCHAMPHELAIRE,[†]
THE HAI PHAM,[†] PASCAL BOECKX,[§]
NICO BOON,[†] AND WILLY VERSTRAETE^{*,†}

Laboratory of Microbial Ecology and Technology (LabMET), Ghent University, Coupure Links 653, B-9000 Ghent, Belgium, Advanced Wastewater Management Centre, University of Queensland, Brisbane, QLD 4072, Australia, and Laboratory of Applied Physical Chemistry (ISOFYS), Ghent University, Coupure Links 653, B-9000 Ghent, Belgium

Microbial fuel cells (MFCs) that remove carbon as well as nitrogen compounds out of wastewater are of special interest for practice. We developed a MFC in which microorganisms in the cathode performed a complete denitrification by using electrons supplied by microorganisms oxidizing acetate in the anode. The MFC with a cation exchange membrane was designed as a tubular reactor with an internal cathode and was able to remove up to 0.146 kg NO₃⁻-N m⁻³ net cathodic compartment (NCC) d⁻¹ (0.080 kg NO₃⁻-N m⁻³ total cathodic compartment d⁻¹ (TCC)) at a current of 58 A m⁻³ NCC (32 A m⁻³ TCC) and a cell voltage of 0.075 V. The highest power output in the denitrification system was 8 W m⁻³ NCC (4 W m⁻³ TCC) with a cell voltage of 0.214 V and a current of 35 A m⁻³ NCC. The denitrification rate and the power production was limited by the cathodic microorganisms, which only denitrified significantly at a cathodic electrode potential below 0 V versus standard hydrogen electrode (SHE). This is, to our knowledge, the first study in which a MFC has both a biological anode and cathode performing simultaneous removal of an organic substrate, power production, and complete denitrification without relying on H₂-formation or external added power.

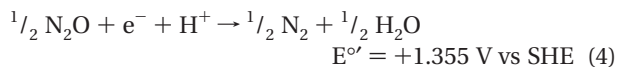
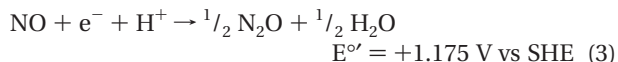
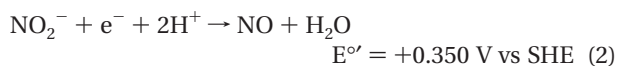
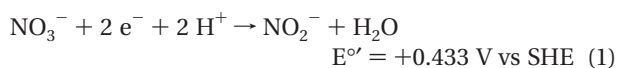
Introduction

Sustainable wastewater treatment not only aims at water reuse but also energy recovery and nutrient management. Similar to anaerobic digestion, where microorganisms produce an energy rich biogas from an organic substrate, energy rich electrons are produced in the anode of a microbial fuel cell (MFC) through microbial catalysis (1). Anodic microorganisms are known to oxidize electron donors such as carbohydrates, volatile fatty acids, and other wastewater compounds (e.g., sulfides) while using an electrode as the sole electron acceptor at a low redox potential (2, 3). Present MFC reactor type systems vary from tubular systems, with an internal (4) or an external cathode (2), to rectangular

configurations that can be easily stacked in order to obtain higher voltages or current outputs (5). For a complete overview of the MFC reactor technology we refer to Logan et al. (6).

The chemical cathodes in the described reactor type MFCs either had an unsustainable cathode system, such as a hexacyanoferrate solution (2), or a relatively expensive platinum cathode for oxygen reduction (7). The latter suffers from poisoning substances originating from the biological activity (e.g., sulfides). Recently, an acid iron solution combined with a bipolar membrane has been successfully tested (8) as well as the use of cobalt tetramethylphenylporphyrin (CoTMPP) (9) as a less expensive and more sustainable cathode. Apart from chemical cathodes, several biological cathodes depending on oxygen as a final electron acceptor have been demonstrated (10, 11). Rhoads et al. (12) described a biological anode delivering electrons to a cathode where manganese oxides were used as electron shuttles to the cathodic biofilm consisting of *Leptothrix discophora*.

It has been demonstrated that *Geobacter* species were able to retrieve electrons directly from a poised graphite electrode without hydrogen formation, and use these electrons to reduce nitrate to nitrite (13). The denitrification of nitrate to nitrite is the first out of four reduction steps (reactions 1–4, standard potentials expressed versus standard hydrogen electrode (SHE) (14) toward nitrogen gas (N₂) using 5 mole electrons per mole of nitrogen.



Also complete cathodic denitrification to nitrogen gas with a chemical anode has been established, however using H₂ as the intermediate reducing agent (15). This hydrogen production required a high energy input (up to 37 V or approximately 1 kWh mol⁻¹ electrons).

In this study, it was our aim to perform a complete cathodic denitrification by microorganisms without any power input but coupled with energy recovery by using a biological anode of a MFC for direct electron delivery. We determined (i) the attainable electricity and power production based on a cathodic denitrification without power input in a continuous cathodic system, and (ii) the operational context in which this denitrification occurred.

Experimental Section

Microbial Fuel Cell Construction. Two identical airtight tubular microbial fuel cells with an internal cathode were constructed (Figure S1 in the Supporting Information). A cation exchange membrane (Ultrex CMI7000, Membranes International Inc., USA), was folded and sealed with superglue to provide a cylindrical cathode compartment with rubber stoppers. This inner cathodic compartment was then surrounded by the anodic compartment, which consisted of a cylindrical Perspex tube and rubber stoppers as outer boundaries. Both the anodic and cathodic compartment were filled with granular graphite (type 00514; diameter 1.5–5 mm,

* Corresponding author phone: +32 (0)9 264 59 76; fax: +32 (0)9 264 62 48; e-mail: Willy.Verstraete@UGent.be; webpage: http://labmet.UGent.be.

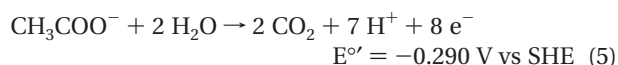
[†] LabMET, Ghent University.

[‡] University of Queensland.

[§] ISOFYS, Ghent University.

estimated projected surface between 817 and 2720 m² m⁻³, Le Carbone, Belgium) and the contact was provided through a graphite rod (5 mm diameter, Morgan, Belgium). The porosity of the graphite bed was 0.55 and the density of the granules was 1.83 kg L⁻¹ (measured values). The volume of the total cathodic compartment (TCC) was 0.444 L while the liquid volume between the graphite granules, the net cathodic compartment (NCC), was 0.244 L. The volume of the total anodic compartment (TAC) was 0.859 L and the volume of the net anodic compartment (NAC) was 0.472 L. The graphite granules (367 g in the cathodic compartment and 708 g in the anodic compartment) were washed at least five times with distilled water before being submerged overnight in turns in 1 N NaOH and 1 N HCl. Afterward the granules were washed five times with distilled water.

Operational Conditions. Both anodic and cathodic liquid streams were recirculated (6 L h⁻¹) in an upflow mode. The anodic liquid stream with an external recirculation vessel consisted of a modified M9 medium (4.4 g KH₂PO₄ L⁻¹, 3.4 g K₂HPO₄ L⁻¹, 2 g NaHCO₃ L⁻¹, 0.5 g NaCl L⁻¹, 0.2 g MgSO₄·7H₂O L⁻¹, 0.0146 g CaCl₂ L⁻¹) and trace elements as previously described (16). Effluent originating from highly performing MFCs was used as an anodic inoculum (5). The reactor was flushed for 30 min with Argon prior to operation. Sodium acetate was the sole electron donor for the anodic oxidation (reaction 5) and was replenished with 1 g of sodium acetate in the anodic recirculation vessel upon depletion.



Acetate depletion was monitored in a fast way by a steep current decrease combined with a high potential of the cathodic electrode. Depletion was then also confirmed by measuring the acetate concentration. The pH in the phosphate buffered anodic liquid decreased slowly and was adjusted with 1 N NaOH to pH 7 when it dropped below 6. The anodic liquid was replaced monthly in order to avoid sodium accumulation (>0.6 g L⁻¹), as the system was operated in batch mode. The cathodic liquid, consisting of the same modified M9 medium but without acetate, was being fed continuously at a rate of 0.650 L d⁻¹. A concentrated KNO₃ solution (2.615 g N L⁻¹) was continuously injected into the cathodic recirculation vessel with a syringe pump at a rate determined by the desired volumetric loading rate (up to 0.160 kg N m⁻³ NCC d⁻¹) and carbonate served as carbon source. Different types of aerobic and anaerobic sludge and sediment were mixed in order to obtain a cathodic inoculum (10 mL) with sufficient microbial diversity. The pH value of the cathodic system remained below 8 except for loading rates higher than 0.109 kg N m⁻³ d⁻¹. In these cases, the pH was adjusted daily to 7 with 5 mL of 1 N HCl. The gas produced was trapped in an external gas collector and the amount of gas produced was monitored daily. The system was operated for more than 8 months without dissolving ammonium in the anodic medium in order to avoid an ammonium flux from the anode to the cathode through the cation exchange membrane (17). All experiments were performed at room temperature (22 ± 2 °C) and in duplicate.

Electrochemical Monitoring. The graphite rod contacts of both the anodic and the cathodic electrode were connected to an external resistance (5–50 Ω) or to a Bi-Stat potentiostat (PAR Bi-Stat Potentiostat, Princeton Applied Research, France). Measurements were performed according to Rabaey et al. (18). During potentiostatic or potentiodynamic measurements the working electrode was always connected with the cathodic electrode and the counter electrode was connected with the anodic electrode. The third electrode was connected to the Ag/AgCl reference electrode (assumed +0.197 V vs SHE) (model RE-5B, BASi, United Kingdom)

within the cathodic electrolyte in the case of a 3 electrode measurement. When applying a fixed cell voltage or a cell polarization (2 electrode measurement), the reference channel of a potentiostat was connected with the counter electrode. The estimation of the ohmic resistance was performed according to the current interrupt method (5). To estimate the contribution of the cathode to the ohmic resistance, the potential of the cathodic electrode was fixed at -0.075 V vs SHE and after stabilization of the current (16 A m⁻³ NCC) the cell was disconnected while a potentiostat recorded (every 10 ms for the first seconds, afterward every 5 s) the potential of the cathodic electrode (working electrode) and the counter electrode.

Calculations. A data acquisition unit (HP 34970A, Agilent, USA) recorded the voltage difference every minute. The hourly averaged values with standard deviation and the value of the external resistance were then used for further calculations. The current and power production were calculated according to Logan et al. (6). The volumetric current density could also be expressed as a theoretical denitrification rate D (kg N m⁻³ NCC d⁻¹) when a complete denitrification occurred:

$$D = \frac{IM}{Fn} \frac{86400 \text{ s d}^{-1}}{1000 \text{ g kg}^{-1}} = 2.507 \times 10^{-3} I$$

with I = the volumetric current density (A m⁻³ NCC), M = the molar mass of nitrogen (14 g N mol⁻¹), F = Faraday's number (96485 C mol⁻¹), and n = the moles of electrons exchanged per mole nitrate reduced (5 for a complete denitrification). N₂O fluxes were calculated assuming 24.47 L mol⁻¹ N₂O (25 °C) and 2.4 × 10⁻² mol L⁻¹ atm⁻¹ as Henry's constant (19). To convert NCC values to TCC values (or NAC to TAC), the porosity was used: NCC TCC⁻¹ = NAC TAC⁻¹ = 0.55. The total MFC volume is the sum of the TAC and the TCC value.

Chemical Analysis. Chemical oxygen demand (COD) and volatile fatty acids were measured (3 times a week for the anodic liquid and once a week for the cathodic effluent) as previously described (16). Cl⁻, NO₂⁻, NO₃⁻, and SO₄²⁻ were determined (daily for cathodic effluent samples and once a week for anodic samples) using an ion chromatograph (Compact IC 761 with conductivity detector, Metrohm, Switzerland) with an metrosep A supp 5 column and a metrosep A 4/5 guard column. A 3.2 mM Na₂CO₃ and 1 mM NaHCO₃ solution was used as eluent at a flow of 0.7 mL min⁻¹. The ammonium concentration was determined according to the colorimetric Nessler procedure (20). N₂O was analyzed with a gas chromatograph (GC-14B, Shimadzu, Japan) fitted with a ⁶³Ni electron capture detector. N₂O was separated from the other gases on a Porapak Q 80–100 mesh column. The carrier gas helium was flowing at 55 mL min⁻¹ and the oven was maintained at 35 °C. The presence of hydrogen gas (H₂) in the headspace of the cathodic recirculation vessel was determined using a H₂ sensor (OPUS, Zellweger Analytics, U.K.). An estimation of the amount of biomass on the cathodic granules was performed after finishing the experiments. All cathodic granules of a reactor were mixed and two samples of 10 g each were taken from each reactor. The graphite granules were vortexed in distilled water until additional vortexing did not give rise to additional biomass detachment, as verified by measuring the concentration of volatile suspended solids (VSS) versus unused graphite granules according to Greenberg et al. (20). The VSS of the detached biomass was determined versus unused graphite granules as a control.

Results

Enrichment Procedure. During the start-up period both reactors were operated with an external resistance of 50 Ω.

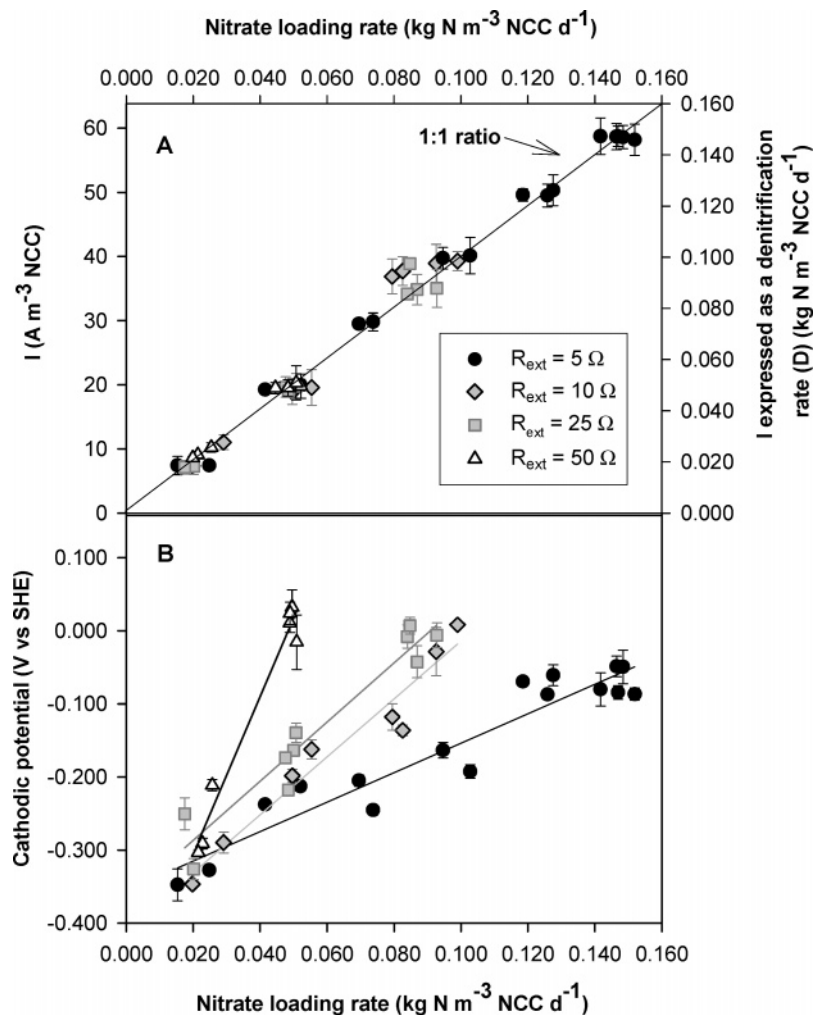


FIGURE 1. Evolution of the current production (A) and the potential of the cathodic electrode (B) at different external resistances in function of the nitrate loading rate. In all cases complete denitrification occurred. The Pearson-correlation coefficients (r^2) for the linear fits in B: for $R = 5 \Omega$, 0.91 ($n = 16$); for $R = 10 \Omega$, 0.95 ($n = 8$); for $R = 25 \Omega$, 0.92 ($n = 10$); for $R = 50 \Omega$, 0.97 ($n = 7$).

The sole electron donor for the anodic consortium was acetate. The sole electron acceptor for the cathodic consortium was nitrate, which was continuously supplied at a loading rate of $0.050 \text{ kg NO}_3^- \text{-N m}^{-3} \text{NCC d}^{-1}$. After approximately a month, both reactors were able to perform a complete denitrification without nitrite accumulation whereas nitrate and nitrite were not completely removed in the start-up period (data not shown). This complete denitrification corresponded with an electrical current production of $19 \pm 1 \text{ A m}^{-3} \text{NCC}$. No hydrogen could be detected in the headspace of the cathodic recirculation vessel. No sulfate reduction was observed in the cathode, as verified by sulfate measurements.

Effect of a Fixed Resistor at Different Nitrate Loading Rates on the Denitrification Activity. Using the enriched culture, the current production, which could also be expressed as a denitrification rate (D), was monitored at different nitrate loading rates and at different external resistances (Figure 1A). The optimal power production was obtained with an external resistance of 25Ω . However, a higher current production was obtained by decreasing the external resistance. Generally, when applying a fixed external resistance, the potential of the cathodic electrode increased with an increasing loading rate of nitrate (Figure 1B).

Aside from nitrate and nitrite removal and current production, the denitrification was verified by measuring N_2O and NH_4^+ formation and quantification of the gas production. The average concentration of N_2O in the head-

space of the cathodic recirculation vessel (0.250 L) was $11.4 \pm 9.7 \text{ ppmv}$, which equals an average content of $3.3 \pm 2.8 \mu\text{g N}_2\text{O-N}$ in this headspace. The gas residence time was between 3 and 25 days, depending on the denitrification rate. According to Henry's law (19) the N_2O removal via the cathodic effluent was calculated to be $5.0 \pm 4.3 \mu\text{g N}_2\text{O-N d}^{-1}$. The nitrogen fed as nitrate to the system was between $4.3 \text{ mg NO}_3^- \text{-N d}^{-1}$ and $37.5 \text{ mg NO}_3^- \text{-N d}^{-1}$ so the N_2O production represented less than 0.3% on the N added. The average ammonium concentration in the effluent was $0.1 \pm 0.2 \text{ mg NH}_4^+ \text{-N L}^{-1}$. The highest ammonium efflux observed was $0.5 \text{ mg NH}_4^+ \text{-N d}^{-1}$ at a nitrogen loading rate of $37.5 \text{ mg NO}_3^- \text{-N d}^{-1}$ (1.4% of added N). The averaged ammonium concentration in the anode was $0.6 \pm 0.7 \text{ mg NH}_4^+ \text{-N L}^{-1}$, though no ammonium was being supplied. The gas production was proportional to the denitrification rate (data not shown). No acetate nor other volatile fatty acids were detected in the cathodic liquid and the averaged chemical oxygen demand (COD) in the cathodic effluent was $16 \pm 5 \text{ mg COD L}^{-1}$.

Effect of a Fixed Cell Voltage at Different Nitrate Loading Rates on the Denitrification Activity. With the use of a potentiostat, different cell voltages were controlled while the current and the evolving potential of the cathodic electrode were monitored until a steady value could be obtained for at least 1 h. This was repeated with different nitrate loading rates. At low controlled cell voltages, a proportional rise in the current was monitored with an increasing loading rate

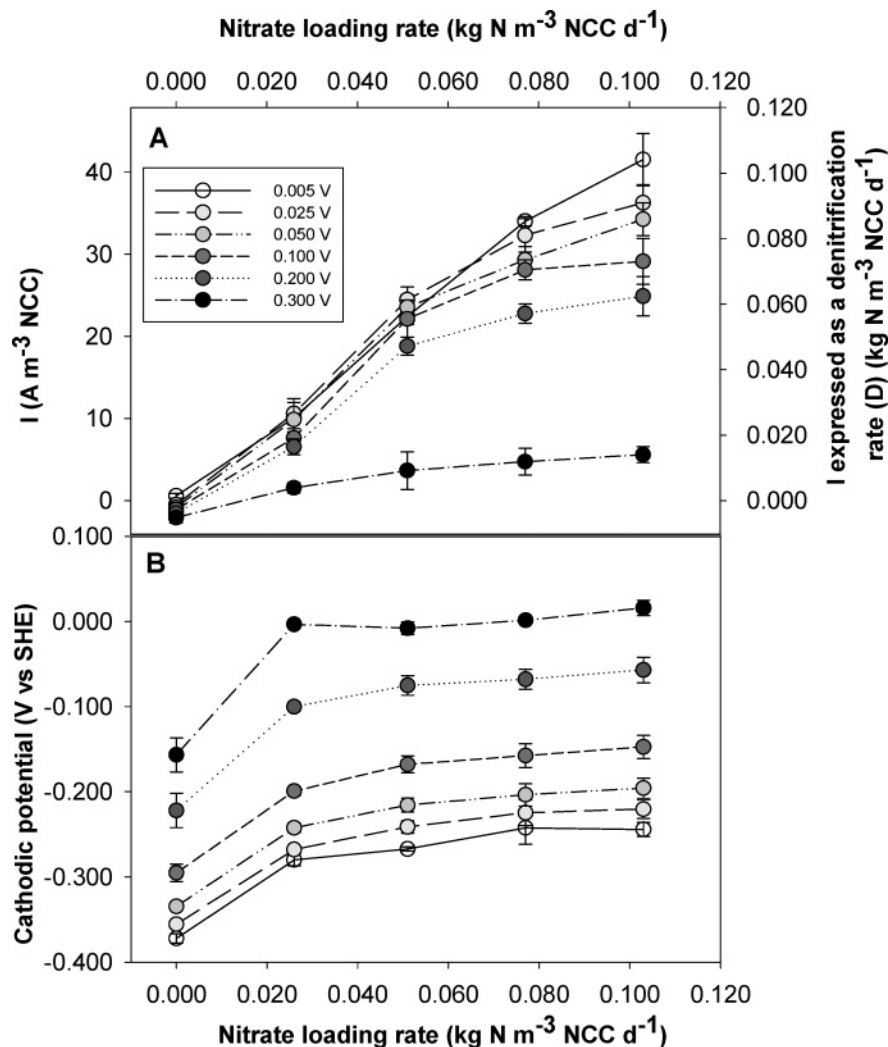


FIGURE 2. Average current production (A) and the potential of the cathodic electrode (B) at different controlled cell voltages in function of the nitrate loading rate.

of nitrate, but at higher controlled cell voltages combined with higher nitrate loading rates the current production decreased, indicating an incomplete denitrification (Figure 2A). With a fixed loading rate of nitrate, an increase of the total cell voltage resulted in an increase of the potential of the cathodic electrode (Figure 2B) and at these higher potentials the denitrification became incomplete. After adaptation to a complete denitrification at different nitrate loading rates forward polarization curves were performed with a potentiostat at a scan rate of 1 mV s^{-1} (Figure 3). Applying a higher nitrate loading rate resulted in a higher power and current production which indicates that the denitrification activity and the power producing capacity of the cell could indeed be increased by adaptation.

Estimation of the Ohmic and Activation Losses. The open cell voltage was typically between 0.300 and 0.360 V when nitrate was being supplied to the cathodic system. The open cell voltage (OCV) of the system, when the same medium but no nitrate was dosed, was $0.005 \pm 0.001 \text{ V}$. The ohmic resistance of the total cells was measured 5 times as described previously (5) for each reactor over a period of 6 months and was $3.9 \pm 0.9 \Omega$ (loading rate: $0.050 \text{ kg NO}_3^- \text{-N m}^{-3} \text{ NCC d}^{-1}$). To estimate the contribution of the cathode to the ohmic resistance, the potential of the working and counter electrode were monitored during a current interrupt test. The potential of the cathodic electrode immediately increased with 0.003 V after disconnecting the cell, the counter electrode showed an immediate decrease of 0.015 V. This corresponds with an

ohmic loss of 0.8Ω in the cathodic electrode and electrolyte and 3.7Ω in the rest of the cell. Within 20 min, the potential of the cathodic electrode increased gradually with 0.115 V (-0.070 V vs SHE to $+0.045 \text{ V vs SHE}$). The counter electrode decreased with another 0.018 V within 2 min and remained steady (Figure S2 of the Supporting Information). These findings indicate that overpotentials at the cathode appear to be considerable.

Poised Cathodic Potential Tests. Using a 3 electrode potentiostat with the reference electrode in the cathodic electrolyte, a cycle of decreasing poised potentials was imposed on the cathodic electrode while the current was recorded. Generally, approximately 30 min was required to obtain a stable current. Decreasing the potential of the cathodic electrode resulted in an increase of the current production. Especially in the potential range of $+0.050$ to -0.030 V vs SHE a steep increase of the current was observed (Figure S3 of the Supporting Information).

Microbial Involvement in the Cathodic Denitrification. Since the cathodic compartment could not be opened for a representative sample of graphite granules during operation, samples from the effluent of both denitrifying cathodes were taken to be investigated with denaturing gradient gel electrophoresis (DGGE) (Figure S4 of the Supporting Information). The Pearson correlation factor between the cathodic systems of both reactors was 71.6%. After finishing the experiments, the reactor was opened and the amount of biomass on the graphite granules, that could be detached by

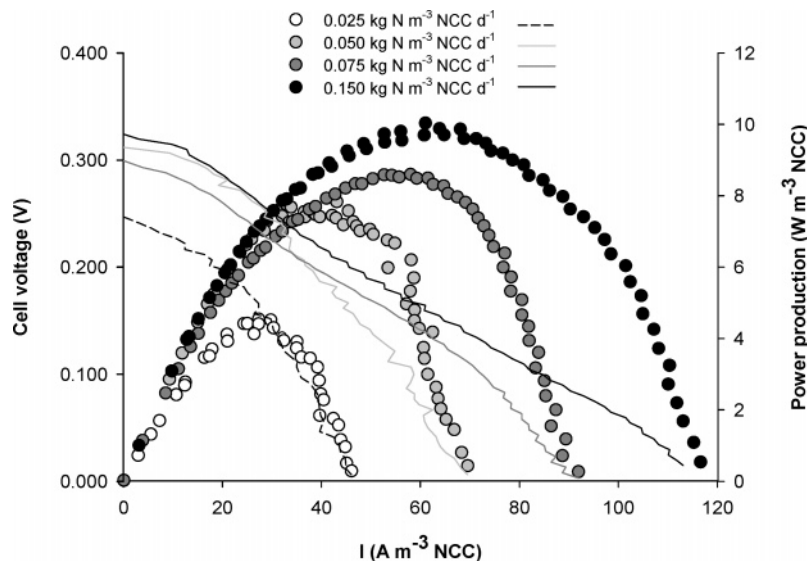


FIGURE 3. Polarization curves (1 mV s^{-1}) at different nitrate loading rates (circles for the power production and lines for the cell voltage).

vortexing, was $0.45 \pm 0.02 \text{ mg VSS g}^{-1}$ cathodic granules. The specific denitrification rate based on this amount of biomass and the volumetric denitrification rate just before opening the reactor was $37 \pm 2 \text{ mg NO}_3^- \text{-N g}^{-1} \text{ VSS d}^{-1}$. The negative control, a cathodic electrode without microorganisms, poised at -0.150 V vs SHE with a potentiostat, did not allow current production when nitrate was supplied (data not shown).

Discussion

Complete Biological Denitrification in the Cathode of a MFC can be Achieved with the Support of a Biological Anode. In this study we have demonstrated that no externally applied electrical energy was needed to drive the anodic nor the cathodic process; instead the combination of these two spontaneous processes delivered electrical energy in a MFC. Only trace amounts of secondary products like ammonium and N_2O were detected. The standard deviation was relatively high since the concentrations of ammonium and N_2O were around the detection limit. The current production was proportional to the denitrification rate (Figure 1A), so it can be concluded that the electron balance corresponded with the nitrogen balance: 5 mole electrons were consumed per mole nitrogen. As previously described for nitrate to nitrite reduction (13), the biological involvement in the denitrification process was found to be essential. The cathodic reduction of nitrate did not occur at a poised abiotic cathode potential (-0.150 V vs SHE). The fact that incomplete denitrification occurred during the start-up period further corroborates these findings. The observation that the DGGE pattern of the effluent of both cathodic systems had a similar composition (Pearson correlation factor of 71.6%) is an indication that the cathodic systems selected for similar microorganisms. However, the conduit through which microorganisms retrieve electrons from the cathodic electrode remains unknown. Further research is needed to reveal whether similar mechanisms, as found for anodes (outer membrane cytochromes (21), electron shuttles (22), or nanowires (23, 24)), are active.

Hydrogen is Not Needed to Drive a Complete Cathodic Denitrification. No hydrogen could be detected in the headspace of the cathodic recirculation vessel, which confirmed previous findings that H_2 production at a graphite electrode is not significant in the potential range of this study (13). The highest obtained denitrification rate in this study ($0.146 \text{ kg NO}_3^- \text{-N m}^{-3} \text{ NCC d}^{-1}$ or $0.080 \text{ kg NO}_3^- \text{-N m}^{-3} \text{ TCC d}^{-1}$) went beyond results obtained by Gregory et al. (13), in a poised biological cathode without H_2 formation. They

TABLE 1. Maximal Power Production Obtained with Different External Resistances in the Case of Complete Denitrification

external resistance (Ω)	nitrate loading rate ($\text{kg N m}^{-3} \text{ NCC d}^{-1}$)	maximal power production ($\text{W m}^{-3} \text{ NCC}$)
5	0.152	4
10	0.099	4
25	0.093	8
50	0.052	5

obtained a denitrification rate in the order of $0.020 \text{ kg NO}_3^- \text{-N m}^{-3} \text{ TCC d}^{-1}$ when reducing nitrate to nitrite on a graphite electrode with a potentiostat (-0.300 V vs SHE). Park et al. (25), obtained a maximal denitrification rate in the order of $0.018 \text{ kg NO}_3^- \text{-N m}^{-3} \text{ TCC d}^{-1}$ in their biological cathodic denitrification system with an abiotic anode driven by a power supply. Though the theoretical denitrification rate from the applied current ($200 \text{ A m}^{-3} \text{ TCC}$) in the latter case was $0.502 \text{ kg NO}_3^- \text{-N m}^{-3} \text{ TCC d}^{-1}$ (calculated value). It was also unclear to which extent H_2 was produced since there was no information provided on the potential of the cathodic electrode. In the latter case, it was also not clear whether N_2O accumulated in the system. Denitrifying reactor beds, where externally produced H_2 is being supplied, have been described to denitrify in the order of $0.600\text{--}0.700 \text{ kg NO}_3^- \text{-N m}^{-3} \text{ d}^{-1}$ (26), while systems where H_2 is produced at the cathode and consumed by a cathodic biofilm have been described to denitrify at a rate of approximately $0.040\text{--}0.060 \text{ kg N m}^{-3} \text{ TCC d}^{-1}$ (15, 27). In such denitrification systems a significant energy input of up to 1 kWh mol^{-1} electrons (15) was required. In this study, an energy recovery of up to $0.006 \text{ kWh mol}^{-1}$ electrons ($8 \text{ W m}^{-3} \text{ NCC}$ and $35 \text{ A m}^{-3} \text{ NCC}$) was obtained (Table 1). The theoretical energy yield can be estimated from the voltage difference between the standard potentials of the anodic and cathodic reactions (reactions 1–5). The lowest calculated yield is in the case of nitrite reduction ($0.017 \text{ kWh mol}^{-1}$ electrons) while the theoretical N_2O reduction yields the highest energy output ($0.044 \text{ kWh mol}^{-1}$ electrons). As the different cathodic reactions of the denitrification (reactions 1–4) occurred simultaneously, the reaction with the lowest potential, in this case probably the nitrite reduction (reaction 2), is likely to determine the potential of the cathodic electrode.

The Potential of the Cathodic Electrode, and thus the Energy Content of the Electrons at the Cathodic Electrode, Limits the Denitrification Rate. It was noted that the

potential of the cathodic electrode increased with an increasing current production. When maintaining a fixed external resistance, we observed that the current production was proportional to the denitrification rate. So a higher current production with a fixed external resistance was realized by a higher cell voltage according to Ohm's law. We observed that this higher cell voltage was mainly realized by a higher cathodic potential (Figure 2B). In this way the cathodic bacteria were still denitrifying while gaining less energy per mole electrons since the external resistance consumed more energy. Moreover, ohmic losses further increase the difference between the voltage across the membrane (defined as the voltage difference between a cathodic reference electrode and an anodic reference electrode (8)) and the cell voltage at higher currents (8).

As the reduction of nitrogen oxides was negatively affected at potentials higher than approximately 0 V vs SHE (Figure S3 of the Supporting Information), no higher currents and thus denitrification rates could be obtained in this system which typically entailed higher potentials of the cathodic electrode at higher currents. The slow increase of the potential of the cathodic electrode in the range of -0.070 to $+0.045$ V vs SHE during the current interrupt experiment (Figure S2 of the Supporting Information) indicates that kinetic factors limit the denitrification rate under the form of cathodic overpotentials.

To improve the denitrification process, the first focus should be on a high denitrification rate at higher cathodic potentials than those obtained in this study. Research on the electron transfer between the cathodic electrode and microorganisms could reveal whether the potentials at which the biological denitrification occurs can further be increased. Decreasing the ohmic losses, e.g., by changing the reactor design, and the selection of appropriate materials is another strategy to improve the process performance. A better catalysis in the cathode could, e.g., be investigated by incorporation of transition metals in the cathodic electrode.

Hypothesis for Cathodic Driven ATP Formation. For every electron that reaches a cathodic microorganism, a cation, originating from the anode, reaches the microorganism after passage through the cation exchange membrane. According to an as yet unknown mechanism, the electrons are being withdrawn from the cathodic electrode into the electron transport chain (ETC) where they are most likely used to reduce quinone type molecules. All involved denitrification enzymes take up electrons from this common quinone pool to reduce nitrogen oxides while creating proton motive force (PMF) for adenosine 5-triphosphate (ATP) formation (28). Since all the denitrifying enzymes in a microorganism take up electrons from the same quinone pool, we now hypothesize that the denitrification enzyme, which is active at the lowest redox potential, determines the redox state of the quinone pool and thus the potential of the cathodic electrode. The exact redox state of the quinone pool is difficult to determine, but the standard potential (E°) of respiratory quinone molecules used in denitrification processes is typically higher than -0.072 V vs SHE (29). Further research on the enzymatic redox activity of the different denitrifying enzymes in the different microorganisms and their interactions is needed to substantiate this hypothesis.

Future Applications. The advantage of the denitrifying MFC is that it is not only oxidizing (generally carbon based) wastewater compounds in the anode, but also, in an integrated and sustainable way, removing nitrogen in the cathode. Nevertheless nutrient recovery is considered even more sustainable. The described denitrification occurred without the addition of a toxic (methanol) nor explosive and poorly dissolving electron donor (H_2). It is, from an energetic point of view, highly sustainable to use a waste stream (e.g., volatile fatty acids in the effluent of an anaerobic digester)

to remove nitrogen and to recover some energy at the same time. The denitrification rate in this paper is lower than conventional heterotrophic denitrification, but the latter does not allow for energy recovery from the substrate. Autotrophic nitrogen removal by combination of aerobic and anaerobic ammonium oxidizing consortia can also achieve higher loading rates but implies a longer start-up period and it is unable to remove organic carbon (30).

A denitrifying MFC is not competitive relative to its oxygen driven counterpart when it comes to power production, but this is compensated by the added value of removing nitrate. It is a denitrification system that is easy to monitor since the current production and potential of the cathodic electrode provide a detailed status on the microbial activity. This also implies that control of the activity is possible. Further research will need to indicate the longevity of the process, and whether further improvement of the activity can be obtained. The system could be applied in a stacked MFC with a certain amount of compartments reserved for denitrification. As nitrogen will mostly be present in the form of ammonium in waste streams, an external nitrification reactor will be necessary.

Acknowledgments

We thank Greet Van de Velde, Ilse Forrez, Petra Van Damme, Siska Maertens, Siegfried Vlaeminck, and Eric Gillis for the technical assistance. The useful comments of Marc Verhaege, Peter De Schryver, and Tom Defoirdt are kindly acknowledged. This research was funded by a Ph.D grant (IWT grant 51305) of the Institute for the Promotion of Innovation through Science and Technology in Flanders (IWT-Vlaanderen). P.A. is supported by a Flemish IWT grant, L.D.S is supported by a BOF grant (Ghent University), and H.T.P. is supported by a Flemish FWO grant.

Supporting Information Available

Figures dealing with a schematic overview of the setup, the potential of the electrodes during a current interrupt test and with the current production at different poised potentials, as well as the DGGE pattern of the effluent of both denitrifying cathodes. This material is available free of charge via the Internet at <http://pubs.acs.org>.

Literature Cited

- 1) Rabaey, K.; Verstraete, W. Microbial fuel cells: novel biotechnology for energy generation. *Trends Biotechnol.* **2005**, *23*, 291–298.
- 2) Rabaey, K.; Clauwaert, P.; Aelterman, P.; Verstraete, W. Tubular microbial fuel cells for efficient electricity generation. *Environ. Sci. Technol.* **2005**, *39*, 8077–8082.
- 3) Rabaey, K.; VandeSompel, K.; Maignien, L.; Boon, N.; Aelterman, P.; Clauwaert, P.; DeSchampelaire, L.; Pham, H. T.; Vermeulen, J.; Verhaege, M.; et al. Microbial fuel cells for sulfide removal. *Environ. Sci. Technol.* **2006**, *40*, 5218–5224.
- 4) He, Z.; Wagner, N.; Minteer, S. D.; Angenent, L. T. An upflow microbial fuel cell with an interior cathode: assessment of the internal resistance by impedance spectroscopy. *Environ. Sci. Technol.* **2006**, *40*, 5212–5217.
- 5) Aelterman, P.; Rabaey, K.; Pham, H. T.; Boon, N.; Verstraete, W. Continuous electricity generation at high voltages and currents using stacked microbial fuel cells. *Environ. Sci. Technol.* **2006**, *40*, 3388–3394.
- 6) Logan, B. E.; Hamelers, B.; Rozendal, R.; Schroder, U.; Keller, J.; Freguia, S.; Aelterman, P.; Verstraete, W.; Rabaey, K. Microbial fuel cells: methodology and technology. *Environ. Sci. Technol.* **2006**, *40*, 5181–5192.
- 7) Liu, H.; Logan, B. E. Electricity generation using an air-cathode single chamber microbial fuel cell in the presence and absence of a proton exchange membrane. *Environ. Sci. Technol.* **2004**, *38*, 4040–4046.
- 8) terHeijne, A.; Hamelers, H. V. M.; deWilde, V.; Rozendal, R. A.; Buisman, C. J. N. A bipolar membrane combined with ferric iron reduction as an efficient cathode system in microbial fuel cells. *Environ. Sci. Technol.* **2006**, *40*, 5200–5205.

- (9) Zhao, F.; Harnisch, F.; Schroder, U.; Scholz, F.; Bogdanoff, P.; Herrmann, I. Application of pyrolysed iron(II) phthalocyanine and CoTMPP based oxygen reduction catalysts as cathode materials in microbial fuel cells. *Electrochem. Commun.* **2005**, *7*, 1405–1410.
- (10) Blake, R. C.; Howard, G. T.; McGinness, S. Enhanced yields of iron-oxidizing bacteria by in-situ electrochemical reduction of soluble iron in the growth-medium. *Appl. Environ. Microbiol.* **1994**, *60*, 2704–2710.
- (11) Bergel, A.; Feron, D.; Mollica, A. Catalysis of oxygen reduction in PEM fuel cell by seawater biofilm. *Electrochem. Commun.* **2005**, *7*, 900–904.
- (12) Rhoads, A.; Beyenal, H.; Lewandowski, Z. Microbial fuel cell using anaerobic respiration as an anodic reaction and biomineralized manganese as a cathodic reactant. *Environ. Sci. Technol.* **2005**, *39*, 4666–4671.
- (13) Gregory, K. B.; Bond, D. R.; Lovley, D. R. Graphite electrodes as electron donors for anaerobic respiration. *Environ. Microbiol.* **2004**, *6*, 596–604.
- (14) Thauer, R. K.; Jungermann, K.; Decker, K. Energy conservation in chemotrophic anaerobic bacteria. *Bacteriol. Rev.* **1977**, *41*, 100–180.
- (15) Sakakibara, Y.; Kuroda, M. Electric prompting and control of denitrification. *Biotechnol. Bioeng.* **1993**, *42*, 535–537.
- (16) Rabaey, K.; Ossieur, W.; Verhaege, M.; Verstraete, W. Continuous microbial fuel cells convert carbohydrates to electricity. *Water Sci. Technol.* **2005**, *52*, 515–523.
- (17) Rozendal, R. A.; Hamelers, H. V. M.; Buisman, C. J. N. Effects of membrane cation transport on pH and microbial fuel cell performance. *Environ. Sci. Technol.* **2006**, *40*, 5206–5211.
- (18) Rabaey, K.; Lissens, G.; Siciliano, S. D.; Verstraete, W. A microbial fuel cell capable of converting glucose to electricity at high rate and efficiency. *Biotechnol. Lett.* **2003**, *25*, 1531–1535.
- (19) Wilhelm, E.; Battino, R.; Wilcock, R. J. Low-pressure solubility of gases in liquid water. *Chem. Rev.* **1977**, *77*, 219–262.
- (20) Greenberg, A.; Clesceri, L. S.; Eaton, A. D. *Standard Methods for the Examination of Water and Wastewater*, 18th ed.; American Public Health Association: Washington, DC, 1992.
- (21) Bond, D. R.; Lovley, D. R. Electricity production by *Geobacter sulfurreducens* attached to electrodes. *Appl. Environ. Microbiol.* **2003**, *69*, 1548–1555.
- (22) Rabaey, K.; Boon, N.; Siciliano, S. D.; Verhaege, M.; Verstraete, W. Biofuel cells select for microbial consortia that self-mediate electron transfer. *Appl. Environ. Microbiol.* **2004**, *70*, 5373–5382.
- (23) Gorby, Y. A.; Yanina, S.; McLean, J. S.; Rosso, K. M.; Moyles, D.; Dohnalkova, A.; Beveridge, T. J.; Chang, I. S.; Kim, B. H.; Kim, K. S.; et al. Electrically conductive bacterial nanowires produced by *Shewanella oneidensis* strain MR-1 and other microorganisms. *PNAS* **2006**, *103*, 11358–11363.
- (24) Reguera, G.; McCarthy, K. D.; Mehta, T.; Nicoll, J. S.; Tuominen, M. T.; Lovley, D. R. Extracellular electron transfer via microbial nanowires. *Nature* **2005**, *435*, 1098–1101.
- (25) Park, H. I.; Kim, D. K.; Choi, Y. J.; Pak, D. Nitrate reduction using an electrode as direct electron donor in a biofilm-electrode reactor. *Process Biochem.* **2005**, *40*, 3383–3388.
- (26) Chang, C. C.; Tseng, S. K.; Huang, H. K. Hydrogenotrophic denitrification with immobilized *Alcaligenes eutrophus* for drinking water treatment. *Bioresour. Technol.* **1999**, *69*, 53–58.
- (27) Feleke, Z.; Araki, K.; Sakakibara, Y.; Watanabe, T.; Kuroda, M. Selective reduction of nitrate to nitrogen gas in a biofilm-electrode reactor. *Water Res.* **1998**, *32*, 2728–2734.
- (28) Zumft, W. G. Cell biology and molecular basis of denitrification. *Microbiol. Mol. Biol. Rev.* **1997**, *61*, 533–616.
- (29) Richardson, D. J. Bacterial respiration: a flexible process for a changing environment. *Microbiol. (UK)* **2000**, *146*, 551–571.
- (30) Pynaert, K.; Smets, B. F.; Beheydt, D.; Verstraete, W. Start-up of autotrophic nitrogen removal reactors via sequential biocatalyst addition. *Environ. Sci. Technol.* **2004**, *38*, 1228–1235.
- (31) Boon, N.; Goris, J.; De Vos, P.; Verstraete, W.; Top, E. M. Bioaugmentation of activated sludge by an indigenous 3-chloroaniline-degrading *Comamonas testosteroni* strain, I2gfp. *Appl. Environ. Microbiol.* **2000**, *66*, 2906–2913.
- (32) Boon, N.; De Windt, W.; Verstraete, W.; Top, E. M. Evaluation of nested PCR-DGGE (denaturing gradient gel electrophoresis) with group-specific 16S rRNA primers for the analysis of bacterial communities from different wastewater treatment plants. *FEMS Microbiol. Ecol.* **2002**, *39*, 101–112.

Received for review October 27, 2006. Revised manuscript received February 23, 2007. Accepted February 26, 2007.

ES062580R